# Effect of precipitating agent NaOH on the preparation of copper oxide nanostructures for electrochemical applications

M. Balasubramaniam, S. Balakumar

National Centre for Nanoscience and Nanotechnology, University of Madras,
Guindy campus, Chennai – 600 025, India

balasuga@yahoo.com

Copper oxide (CuO) nanostructures with different concentrations of sodium hydroxide for electrochemical applications such as supercapacitors have been synthesized using a simple and low-cost precipitation method. X-ray diffraction pattern confirmed the formation of CuO nanostructures without any impurities and further confirmed its highly crystalline, single phase, monoclinic nature. UV-diffuse reflectance spectral (UV-DRS) studies provided the absorption edge of the material and the estimated band gap value for the nanostructures were calculated using Kubelka-Munk (KM) absorbance plot that are determined to be around 4.74 – 4.84 eV. Field emission scanning electron microscopy (FESEM) investigations revealed the morphology of the copper oxide nanocrystals and showed the increment of diameter of the CuO nanostructures. The electrochemical behavior of the CuO nanostructures were investigated using electrochemical impedance spectroscopy (EIS) and cyclic voltammetry (CV) techniques which showed the stability, reversibility, symmetric and capacitive nature of the nanostructures.

Keywords: copper oxide nanostructures, sodium hydroxide, electrochemical behavior, capacitive nature, stability.

Received: 23 January 2016. Revised: 18 April 2016

## 1. Introduction

In recent years, considerable research has been done to develop nanostructured materials for supercapacitors by virtue of their exclusive properties such as high specific surface area, shorter ion diffusion, and electrochemical activity [1–5]. Ruthenium Oxide ($RuO_2$) and Iridium Oxide ($IrO_2$) of noble metal oxide materials were used as pseudocapacitive electrode materials with extraordinary performance [6, 7]. However, the high cost of hydrous $RuO_2$ and $IrO_2$ hindered their wide application. Consequently, increasing interest has been generated for the use of cheap transition metal oxides, such as nickel oxide (NiO) [8], cobalt oxide ($Co_3O_4$) [9], vanadium oxide ($V_2O_5$) [10], manganese oxide ($MnO_2$) [11], and copper oxide (CuO) [12]. Of these, CuO has attracted much research interest due to its unique properties, such as high catalytic activity, easy synthesis route, environmentally friendly nature and variable morphologies at the nanoscale. It has found potential applications in electrochemistry as an electrode material for lithium-ion batteries and electrochemical capacitors, solar energy systems, heterogeneous catalysts and selective gas sensors [13, 14]. CuO is a metal oxide with encouraging redox properties, and thus thin CuO films fabricated by different techniques such as electrodeposition [15] and chemical bath deposition [16] can find certain use in supercapacitors. However, the highest specific capacitances obtained in those studies are only 37 and 43 $F \cdot g^{-1}$, respectively [15, 16]. The low capacitances may be due to the film morphology with a poorly-accessible surface area. It is also difficult for the ions and electrons to diffuse through a submicron-thick film. To overcome the above-mentioned drawbacks, it is necessary to prepare different CuO nanostructures in order to create well-dispersed and an increased number of active sites that can interact with ions and the electrolyte. Furthermore, the different morphologies of CuO have been shown to have effects on the optical, semiconducting, and piezoelectric properties. In this study, we report the preparation of various CuO nanostructures using different molar concentrations of precipitating agent, sodium hydroxide by simple precipitation method. The obtained CuO nanostructures were characterized using XRD, FESEM, and UV-DRS techniques. Also, the electrochemical behaviors of CuO nanostructures for supercapacitors were investigated using EIS and CV studies.

## 2. Materials and Methods

Copper acetate monohydrate ($Cu(CH_3COO)_2 \cdot H_2O$, Merck), sodium hydroxide (NaOH, Merck) and double distilled water were used in the preparation. All the chemicals were of analytical grade. A calculated amount of copper acetate monohydrate was added in 20 ml of double distilled water, after complete dissolving of the precursor material in the solvent, precipitating agent sodium hydroxide (NaOH) solution at various concentrations such as 1.5 M, 3.0 M, 4.5 M and 5.0 M were added dropwise and the mixture was stirred for 2 h. After 2 h, the color of the solution changed from blue to black with precipitates under the supernatant solution. The precipitates

were filtered, washed with distilled water for several times and dried in a hot air oven at 100 °C for 6 h. The X-ray diffraction (XRD) technique (Model D8 Advance, Rigaku X-ray Diffractometer) was used for structural analysis. Field emission scanning electron microscopy (FE-SEM) (Hitachi SU-6600) was used for the imaging of the morphologies. The optical reflectance and band gap properties were studied using a UV-DRS technique (Perkin Elmer Lambda 650 Spectrophotometer). The electrochemical behaviors of the CuO nanostructures were studied using cyclic voltammetry (CV) and electrochemical impedance spectroscopy (EIS) studies (Bio-logic-science instruments). Cyclic voltammetric and EIS measurements were performed with an electrochemical analyzer in a conventional three electrode cell with glassy carbon electrode (GCE) as a working electrode, on which the CuO sample was coated, Ag/AgCl as the reference electrode and a Pt wire as the counter electrode. All potentials were reported with respect to the Ag/AgCl electrode. KOH (1M) solution was used as an electrolyte.

## 3. Results and discussion

### 3.1. XRD analysis

Figure 1 displays the XRD profiles of the CuO nanostructures synthesized using different concentrations of NaOH. All of the Bragg's reflections can be indexed to the monoclinic-phase [17–19] of CuO (space group C2/c), which is very close to the reported data (JCPDS 48-1548) whereas no characteristic peaks of any other impurities such as $Cu(OH)_2$, $Cu_2O$, or precursors used were observed. In all cases, peak broadening was observed, which depicts the nanostructural crystalline domains in CuO. The average crystallite size was determined using Debye-Scherer's relation which is represented in Table 1. From the $\beta$ values, it is evident that the crystallographic growth was suppressed at 5.0 M NaOH, which is the maximum crystal growth concentration.

TABLE 1. Average crystallite size and FWHM of CuO nanostructures

| Concentration of NaOH | FWHM ($\beta$) | Crystallite size (nm) |
|:---:|:---:|:---:|
| 1.5 M | 0.9194 | ~20 |
| 3.0 M | 0.90133 | ~20.5 |
| 4.5 M | 0.64512 | ~29 |
| 5.0 M | 0.9200 | ~20 |

### 3.2. Optical analysis

Figure 2(a) displays the reflectance spectra of CuO nanostructures prepared at different concentrations of sodium hydroxide. In all the cases, the spectra were recorded with the onset of an absorption edge at 350 nm and it extended toward the UV region of the spectra. The band gap values were estimated using the Kubelka-Munk (K-M) absorption plot shown in Fig. 2(b). The optical band gap values were determined and found to be 4.84, 4.81, 4.76 and 4.74 eV [20] for ultrathin CuO nanorods, thin CuO nanorods, CuO nanorods and CuO nanotubes respectively, which also illustrated that the addition of NaOH on the CuO nanostructures shows remarkable changes in the optical properties. As the diameter of the crystal (ultrathin nanorods) is smaller for the case of 1.5 M NaOH, the band gap value is high (4.84 eV) compared to other nanostructures such as, thin nanorods (4.81 eV), nanorods (4.76 eV) and nanotubes (4.74 eV). The blue shift in optical band gap energy satisfies the quantum confinement effect.

### 3.3. Morphological analysis

NaOH is a strong electrolyte that may neutralize the surface charges of the CuO, thereby preventing them from possible crystalline aggregation. Finally, the use of high concentration NaOH may create diffusion layers on certain surfaces of CuO, which may in turn create an additional growth anisotropy, allowing only energetically favorable crystallographic planes to grow. Fig. 3 shows the FESEM micrographs of CuO nanostructures prepared at 1.5, 3.0, 4.5 and 5.0 M concentrations of NaOH that were imaged at an operating voltage of 15 kV. At 1.5 M NaOH, CuO nanostructures were formed with bundles of ultrathin nanorod morphology with diameters in the range of 7 – 33 nm and rod lengths of 92 – 172 nm. At 3.0 M NaOH, bundles of thin nanorod morphology with diameters in the range of 9 – 35 nm and rod lengths of 88 – 159 nm were observed. At 4.5 M NaOH, bundles of nanorod morphology with diameters in the range of 19.5 – 36 nm and rod lengths of 85 – 151 nm were observed. At 5.0 M NaOH, bundles of nanotube morphology with diameters ranging from 42 – 598 nm and tube lengths of 159 nm to several microns were observed. From the figures, it is evident that the addition of a greater number of OH-ions on the CuO makes the crystal grow along the diameter. In all four nanostructures, quantum confinement exists in
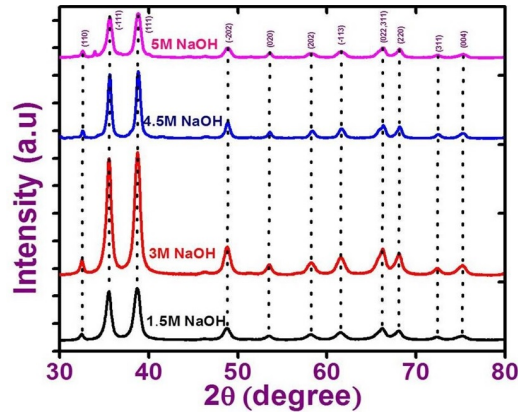
FIG. 1. XRD pattern of CuO nanostructures prepared using different concentrations of NaOH (1.5 M, 3.0 M, 4.5 M and 5.0 M)
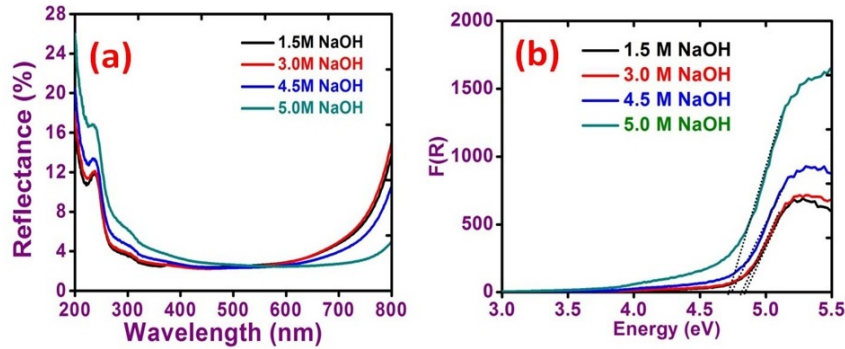


FIG. 2. (a) UV-diffuse reflectance spectra and (b) Kubelka-Munk (K-M) absorbance plot of CuO nanostructures prepared using different concentrations of NaOH (1.5 M, 3.0 M, 4.5 M and 5.0 M)

the diameter axis which is found to be in nanoscale regime and this could be the crucial factor for better capacitor characteristics.

### 3.4. Electrochemical analysis

To investigate the electrochemical behavior of the CuO nanostructures for energy storage devices such as supercapacitors, cyclic voltammetry studies were performed on all four types of CuO nanostructures. Fig. 4(a) exhibits the CV curves of all the CuO nanostructures, electrochemical redox peaks are observed at potentials ranging from 0.1 to 0.4 V. As observed, the CV current response of sample increases gradually with increasing scan rate, indicating reversible redox reaction taking place at the electrode material interface: all CV curves show typical pseudocapacitance behavior. These results also show two main peaks: a broad cathodic peak, and sharp-edged anodic peaks that are corresponding to redox reaction of $Cu^{2+}/Cu$ [21]. Storage mechanism in CuO has been proposed as follows. It is based on the intercalation/extraction of protons in the electrode that is oxidation/reduction of the electrode (surface adsorption and desorption of protons) [21]. When the CuO electrode is swept towards a negative potential, cathodic current flows according to $Cu^{2+} \longleftrightarrow Cu^{+}$ reduction process whereas during a positive potential sweep, anodic current flows due to $Cu^{+} \longleftrightarrow Cu^{2+}$ oxidation process [21]. The net redox reaction can be represented by the equation.

$$Cu^{2+} + e^{-} \longleftrightarrow Cu^{+}.$$
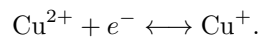
Thus, the CV curves indicated that the nanomaterial has reversibility, is symmetric and has capacitive behavior. Even though all the samples are prepared at different concentrations of NaOH, all the CV curves exhibit similar pattern in shape that evidently confirmed the electrochemical stability of the nanostructure at different NaOH concentrations. In addition, the specific capacitance value was calculated for all the four samples by using the relation (1) and the values are tabulated in Table 2:

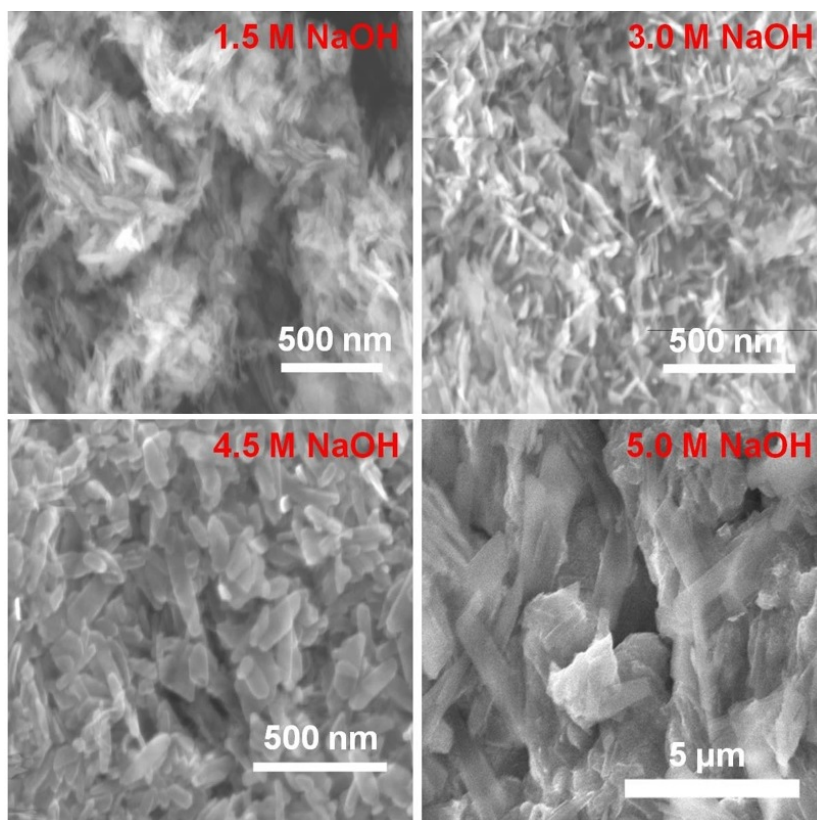$$C_s = \frac{1}{mS} \times \text{area of integration.} \tag{1}$$

FIG. 3. FESEM micrographs of CuO nanostructures prepared using different concentrations of NaOH (1.5 M, 3.0 M, 4.5 M and 5.0 M)

TABLE 2. Specific capacitance of CuO nanostructures at different scan rates

| Samples | Scan rate (mV/s) | Specific Capacitance (F/g) |
|---------|------------------|----------------------------|
| 1.5 M | 20 | 753.34 |
|  | 50 | 426.34 |
|  | 100 | 338.26 |
| 3.0 M | 20 | 759.51 |
|  | 50 | 450.48 |
|  | 100 | 322.70 |
| 4.5 M | 20 | 640.32 |
|  | 50 | 297.28 |
|  | 100 | 300.0 |
| 5.0 M | 20 | 667.82 |
|  | 50 | 385.97 |
|  | 100 | 305.06 |

The electrochemical studies evidently confirms that the CuO nanostructures prepared by using simple precipitation method shows better capacitive performance with high specific capacitance values, which may be due to two major reasons: (1) high specific surface area and (2) the diameter in all four nanostructures is found to be in the nanoscale regime and the aggregation effects are also minimal, so the electrolyte ions can migrate or diffuse easily between the structures and access the active sites in CuO nanostructures and also the smaller particles have better accessibility and mobility towards OH- ions from the electrolyte thereby resulting in a higher capacitance value.
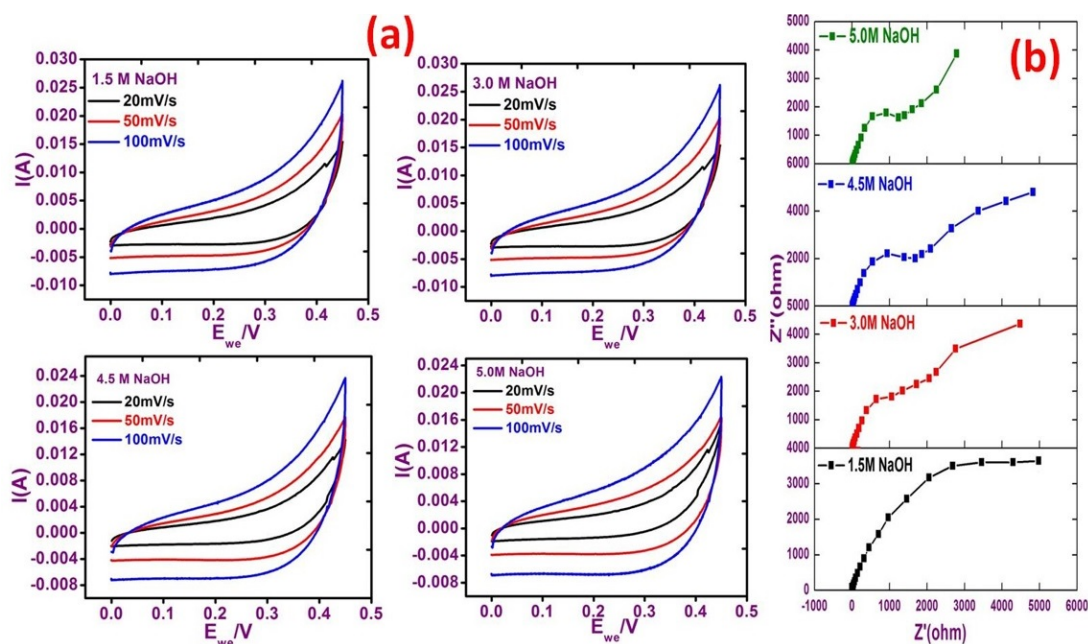
FIG. 4. (a)Typical cyclic voltammograms and (b) Nyquist plots of CuO nanostructures prepared using different concentrations of NaOH (1.5 M, 3.0 M, 4.5 M and 5.0 M) at different scan rates (20, 50 and 100 mV/s) in 1 M KOH solution

The specific capacitance was found to be significantly higher than the reported values [21]. Hence, the CuO nanostructures prepared by this simple approach would contribute as a cheap and efficient metal oxide supercapacitor electrode material.

Also, to better determine the nanostructure among the four different nanostructures for electrochemical capacitor applications, EIS studies were carried out. EIS is an excellent tool used to explore the electrochemical characteristics of electrode/electrolyte interface using a Nyquist plot. The main purpose of the EIS experiments is to study the effect of NaOH on the interfacial properties of CuO electrodes (capacitance and electron charge transfer resistance). The Nyquist plot of the four prepared electrodes is shown in Fig. 4(b). In all four samples, a partial semicircle in the high-frequency region corresponding to the electron charge transfer resistance due to the Faradaic redox process at the electrode/electrolyte interface was observed. This resistance is associated with two resistances: electrolyte resistance and the material (oxide) resistance which arises from the non-uniform continuity in the charge transfer process at the electrode/electrolyte interface because of the conductivity differences between the oxide (CuO) and the electrolyte [22]. A line is observed in the low frequency region corresponding to electron-transfer diffusion process. It is worth stating that for ideal electrochemical capacitors, the plot should be a line perpendicular to the real axis at low frequency region. A comparison of the low frequency region in all four samples reveals that the 5.0 M NaOH made CuO nanostructure that shows the best electron diffusion process in comparison to the other three nanostructures. Thus, we conclude that the CuO nanotubes (5.0 M NaOH) are a better nanostructure for electrochemical applications.

## 4. Conclusion

In summary, CuO nanostructures were synthesized by varying the concentration of NaOH for electrochemical capacitor applications using a facile precipitation method. The XRD pattern confirmed the formation of CuO nanostructures without any impurities and further confirmed the highly crystalline, single phase, monoclinic nature of the CuO nanostructures. UV-DRS spectra confirmed the absorption edge of the material and the band gap values were estimated using Kubelka-Munk absorbance plot and were in the range of 4.74 to 4.84 eV. The FESEM investigations revealed that the addition of $OH^-$ ions increased the diameter of the CuO crystals. The electrochemical behavior was studied using CV and EIS techniques that exhibited the stability, reversibility, symmetric and capacitive nature of the nanostructures. Among the CuO nanostructures, the nanotubes were found to have good electron diffusion activity than the other nanostructures that was evident from the EIS curves. The study finally concluded that the CuO nanostructures can be used as a potential electrode material for supercapacitor applications.

## Acknowledgement

## References

[1] Rakhi R.B., Chen W., Cha D., Alshareef H.N. Substrate dependent self-organization of mesoporous cobalt oxide nanowires with remarkable pseudocapacitance. *Nano Letters*, 2012, **12**, P. 2559–2567.

[2] Wang H., Holt C. et al. Graphene-nickel cobaltite nanocomposite asymmetrical supercapacitor with commercial level mass loading. *Nano Research*, 2012, **5**, P. 605–617.

[3] He X., Li R., et al. Synthesis of mesoporous carbons for supercapacitors from coal tar pitch by coupling microwave-assisted KOH activation with a MgO template. *Carbon*, 2012, **50**, P. 4911–4921.

[4] Chen C.Y., Shih Z.Y., Yang Z., Chang H.T. Carbon nanotubes/cobalt sulfide composites as potential high-rate and high-efficiency supercapacitors. *Journal of Power Sources*, 2012, **215**, P. 43–47.

[5] Song M.K., Cheng S., et al. Correction to Anomalous Pseudocapacitive Behavior of a Nanostructured, Mixed-Valent Manganese Oxide Film for Electrical Energy Storage. *Nano Letters*, 2012, **12**, P. 3483–3490.

[6] Terasawa N., Mukai K., Asaka K. Superior performance of a vapor grown carbon fiber polymer actuator containing ruthenium oxide over a single-walled carbon nanotube. *Journal of Materials Chemistry*, 2012, **22**, P. 15104–15109.

[7] Murakami Y., Nakamura T., Zhang X.G., Takasu Y. Preparation of highly porous iridium oxide electrodes by pore initiation with rare earth ions. *Journal of Alloys and Compounds*, 1997, **259**, P. 196–199.

[8] Zhang Y.Q., Xia X.H., et al. Self-assembled synthesis of hierarchically porous NiO film and its application for electrochemical capacitors. *Journal of Power Sources*, 2012, **199**, P. 413–417.

[9] Zhang F., Yuan C., et al. Facile growth of mesoporous $Co_3O_4$ nanowire arrays on Ni foam for high performance electrochemical capacitors. *Journal of Power Sources*, 2012, **203**, P. 250–256.

[10] Ghosh A., Ra E.J., et al. High Pseudocapacitance from Ultrathin $V_2O_5$ Films Electrodeposited on Self-Standing Carbon-Nanofiber Paper. *Advanced Functional Materials*, 2011, **21**, P. 2541–2547.

[11] Dong M., Zhang Y.X., et al. Self-assembled spongy-like $MnO_2$ electrode materials for supercapacitors. *Physica E*, 2012, **45**, P. 103–108.

[12] Sun G., Li K., et al. Physical and electrochemical characterization of CuO-doped activated carbon in ionic liquid. *Electrochimica Acta*, 2010, **55**, P. 2667–2672.

[13] Shaikh J.S., Pawar R.C., et al. CuO-PAA hybrid films: Chemical synthesis and supercapacitor behavior. *Applied Surface Science*, 2011, **257**, P. 4389–4397.

[14] Xiang J.Y., Tu J.P., et al. Self-assembled synthesis of hierarchical nanostructured CuO with various morphologies and their application as anodes for lithium ion batteries. *Journal of Power Sources*, 2010, **195**, P. 313–319.

[15] Patake V.D., Joshi S.S., Lokhande C.D., Joo O.S. Electrodeposited porous and amorphous copper oxide film for application in supercapacitor. *Materials Chemistry and Physics*, 2009, **114**, P. 6–9.

[16] Dubal D.P., Dhawale D.S., et al. Fabrication of copper oxide multilayer nanosheets for supercapacitor application. *Journal of Alloys Compounds*, 2010, **492**, P. 26–30.

[17] Aixia Gu, Guangfeng Wang, Xiaojun Zhang, Bin Fang. Synthesis of CuO nanoflower and its application as a $H_2O_2$ sensor. *Bulletin of Materials Science*, 2010, **33**, P. 17–20.

[18] Anita Sagadevan Ethiraj, Dae Joon Kang. Synthesis and characterization of CuO nanowires by a simple wet chemical method. *Nanoscale Research Letters*, 2012, **7**, P. 70.

[19] Volanti D.P., Keyson D., et al. Synthesis and characterization of CuO flower-nanostructure processing by a domestic hydrothermal microwave. *Journal of Alloys and Compounds*, 2008, **459**, P. 537–542.

[20] Han Ho Choi, Joodong Park, Singh R.K. Nanosized CuO Encapsulated Silica Particles Using an Electrochemical Deposition Coating. *Electrochemical and Solid-state Letters*, 2004, **7**, P. C10–C12.

[21] Bello A., Dodoo-Arhin D., et al. Surfactant Assisted Synthesis of Copper Oxide (CuO) Leaf-like Nanostructures for Electrochemical Applications. *American Journal of Materials Science*, 2014, **4**, P. 64–73.

[22] Meher S.K., Justin P., Rao G.R. Microwave-Mediated Synthesis for Improved Morphology and Pseudocapacitance Performance of Nickel Oxide. *ACS Applied Materials & Interfaces*, 2011, **3**, P. 2063–2073.